Brief Articles

Role of the Hydrogen Bonding Heteroatom−Lys53 Interaction between the p38α Mitogen-Activated Protein (MAP) Kinase and Pyridinyl-Substituted 5-Membered Heterocyclic Ring Inhibitors

Bassam Abu Thaher,[†] Pierre Koch,[‡] Verena Schattel,[‡] and Stefan Laufer*[,‡]

Faculty of Science, Chemistry Department, Islamic University of Gaza, Gaza Strip, Palestine, and Department of Pharmaceutical and Medicinal Chemistry, Institute of Pharmacy, Eberhard-Karls-University of Tübingen, Auf der Morgenstelle 8, 72076 Tübingen, Germany

Received November 21, 2008

In the framework of investigating the role of heteroatoms in pyridinyl-substituted 5-membered (hetero)cycles as potential p38α MAP kinase inhibitor scaffolds, cyclopentene, pyrrole, furan, and imidazole analogues were synthesized and tested with respect to their ability to inhibit p38α MAP kinase. The vicinal pyridine/4-fluorophenyl pharmacophore was conserved, such as in the prototypical imidazole inhibitor SB203580. The strength of the HB interaction was calculated and compared to the biological data.

Introduction

The p38 MAP[a] kinase, a serine/threonine kinase, is one of the best studied kinases in the inflammatory process.[1,2] It is a key-player in the biosynthesis of pro-inflammatory cytokines, such as IL-1β and TNF-α at both the translational and the transcriptional level.[1,3] Activation of this kinase by different extracellular stimuli results in diphosphorylation of Thr180 and Tyr182 in its activation loop.[1,4] Among the four identified p38 isoforms (p38α, p38β, p38γ, and p38δ), the α-form is the fully studied. The structural appearance of the ATP-binding site in protein kinases has been reviewed recently.[5,6] Cocrystallographic data of the isolated p38α MAP kinase complexed with various pyridin-4-yl imidazole derivatives described a common ground of features that can be exemplified by the way SB203580 (**1**) binds to the protein (Figure 1).[4] The ATP competitive inhibitor **1** binds in the ATP binding site located in the cleft between the N- and the C-terminal domains of p38α MAP kinase, making a crucial hydrogen bond (HB) between the pyridin-4-yl moiety and the backbone NH of Met109 in the hinge region. The importance of this HB is deduced from a decrease in activity when the pyridin-4-yl moiety is replaced by a pyridin-3-yl or a phenyl moiety.[7,8] The 4-fluorophenyl ring interacts with the hydrophobic pocket I, mainly causing selectivity, which is mediated by the presence of the gatekeeper residue Thr106 in the ATP-binding site. Another possible ligand−protein interaction is a $\pi-\pi$ stacking between Tyr35 and the phenyl system at the 2-position of the imidazole core of **1**. The hydrophobic region II remains unoccupied by **1**. The relevance of the HB between Lys53 of the p38α MAP kinase and the N-3 of the imidazole core is still unclear. Several studies indicate the imidazole ring-N as a critical determinant for the binding of pyridinyl-imidazoles to the side chain of Lys53.[1,4] Some authors suggest an important role for the imidazole core as a scaffold for positioning the vicinal pyridine/4-fluorophenyl system. For example, Fitzgerald et al. reported no interaction between the side chain nitrogen of Lys53 and the N3 of the imidazole ring of their pyrimidinyl−imidazole compound.[9] Lys53 appears to be too distant for HB interaction to the imidazole ring.[6]

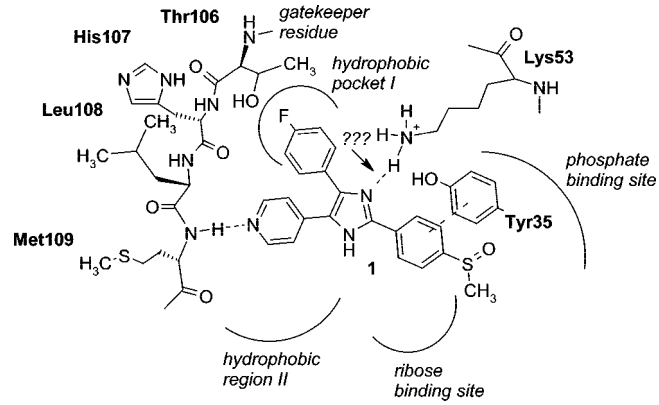

Figure 1. Schematic drawing of important interactions between the competitive inhibitor SB203580 (**1**) and the ATP binding site of p38α.

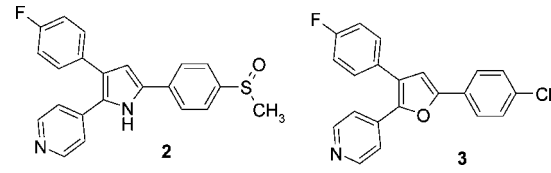

Figure 2. Inhibitors of p38 MAP kinase: cmpd **2** (IC_{50} = 670 nM);[10] cmpd **3** (IC_{50} = 530 nM).[11]

There are compounds with moderate inhibitory activity that are unable to form a HB to Lys53, for example compounds **2**[10] and **3**[11] (Figure 2). The modest inhibitory activity of these compounds, which are unable to form a HB to Lys53, underscored the demand for further investigations.

* To whom correspondence should be addressed. Telephone: +497071-2972459. Telefax: +497071-295037. E-mail: stefan.laufer@uni-tuebingen.de.
† Islamic University of Gaza.
‡ Eberhard-Karls-University of Tübingen.

[a] Abbreviations: ATP, adenosine triphosphate; IL, interleukin; AEPC, atomic electrostatic potential charge; MAP, mitogen-activated protein; NaHMDS, sodium hexamethyldisilazane; HB, hydrogen bond; TNF tumor necrosis factor; d.a., dihedral angle; DTF, density functional theory.

10.1021/jm801467h CCC: $40.75
Published on Web 03/20/2009

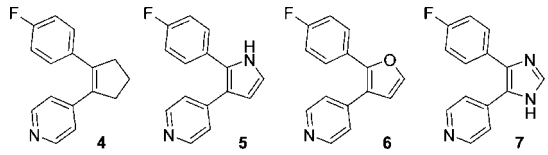

Figure 3. Cyclopentene **4**, pyrrole **5**, furan **6**, and imidazole **7** derivatives.

Table 1. Biological Data of Compounds **4**−**7**

compd	**4**	**5**	**6**	**7**
$IC_{50} \pm SEM^a$ (μM)	4.05 ± 0.67	0.42 ± 0.11	0.74 ± 0.18	0.079 ± 0.006

[a] Results are of three experiments.

A HB [D−H···A] consists of a donor (D−H) and acceptor (A) subunit and plays a very important role in drug design. The strength of a HB ranges from >1 to about 40 kcal/mol[12] and is weaker than a normal covalent bond. A HB dictates the orientation of an inhibitor binding in the receptor and contributes importantly to binding affinity. The major component of hydrogen-bonding interaction is electrostatic.[13,14] Furthermore, the geometry (distance and orientation) between HB-donor and HB-acceptor is important for the strength of the HB. To enhance the hydrogen-bonding interaction in drug discovery, bioisosteric replacement is used.

The aim of this work was to conserve the vicinal pyridinyl/4-fluorophenyl system of the prototypical imidazole **1** while replacing the central imidazole core by a carbocyclic scaffold (cyclopentene **4**, Figure 3) and different bioisosteric heterocyclic scaffolds (pyrrole **5**, furan **6**, imidazole **7**, Figure 3). These compounds can be considered as key compounds to reveal the role of the hydrogen bonding heteroatom−Lys53 interaction.

The difference in interaction of the title compounds **4**−**7** at the ATP-binding cleft of p38α MAP kinase is mainly characterized by the hydrogen bonding interaction between the inhibitor molecule and the amino function of the side chain of Lys53 (Figure 4). Under physiological conditions the side chain of Lys53 is protonated. Therefore, this protonated amino function can only interact as a HB-donor. Between compounds **4** and **5** and Lys53, no HB can be formed. Compounds **6** and **7** can interact with Lys53 by hydrogen bonding interaction. The heteroatom X is the acceptor of the HB, and the amino function of the side chain of Lys53 is the donor of the HB. To estimate the strength of this hydrogen bonding interaction between X and Lys53, the atomic electrostatic potential charges (AEPCs) of analogues **6** and **7** were calculated and the hydrogen binding energies of **6** and **7** to Lys53 were determined by docking experiments with the inhibitors and the p38 MAP kinase.

Chemistry

The synthetic route toward the cyclopentene derivative **4** (Scheme 1) was published recently.[15] Cyclopentanone (**8**) was converted into cyclopentenyl fluorobenzene (**9**) using the Grignard reaction, followed by oxidation with hydrogen peroxide in the presence of formic acid, yielding fluorophenyl cyclopentanone (**10**). This ketone was activated using a neodymium salt ($NdCl_3 \cdot 2LiCl$) and consecutively reacted with the complex Grignard reagent PyMgCl·LiCl, affording the corresponding cyclopentanol derivative **11**. Finally, the dehydration of alcohol **11** with p-TsOH and a few drops of concentrated sulfuric acid in toluene under reflux conditions gave 2-(4-fluorophenyl)-1-(pyridin-4-yl)cyclopentene (**4**).

The pyrrole derivative **5** was synthesized according to a protocol of Qian et al.[16] starting from 1-(4-fluorophenyl)-2-(pyridin-4-yl)ethanone (**12**) (Scheme 2). Ethanone **12** was deprotonated using NaHMDS (2 M in THF) at 0 °C and treated with allylbromide. After quenching the reaction mixture with HCl (2 N) and extraction with ethyl acetate, the crude product was purified by flash chromatography to yield 1-(4-fluorophenyl)-2-(pyridin-4-yl)pent-4-en-1-one (**13**). Ozonolysis of **13** in MeOH at 0 °C, followed by reductive workup of the ozonide with dimethyl sulfide, gave aldehyde **14**. Finally, 2-(4-fluorophenyl)-3-(pyridin-4-yl)-1*H*-pyrrole (**5**) was prepared via Paal−Knoor condensation of the 1,4-dicarbonyl compound **14** by heating it together with ammonium acetate in acetic acid up to 115−120 °C. 2-(4-Fluorophenyl)-3-(pyridin-4-yl)furan (**6**) was prepared by acid catalyzed dehydration of aldehyde **14** (Scheme 2). Therefore, a mixture of **14**, glacial acetic acid, and concentrated HCl was heated to reflux temperature.

A possible synthetic access to 4-(4-fluorophenyl)-5-(pyridin-4-yl)-1*H*-imidazole (**7**) via a modified van Leusen methodology for 1,3-dipolar cycloaddition of the anion of tosylmethyl isocyanides to imines was published in 1996 by Boehm et al.[17] We chose another synthetic strategy for the formation of the imidazole ring (Scheme 3). The imidazole derivative **7** was synthesized starting from 1-(4-fluorophenyl)-2-(pyridin-4-yl)ethanone (**12**). Compound **12** was oxidized by selenium dioxide into the α-diketo compound **15**. The formation of the imidazole ring was accomplished by a microwave-assisted Radziszewski reaction.[18] Treatment of **15**, NH_4OAc, and formaldehyde (37% aq solution) in a microwave synthesizer yielded the 4-(4-fluorophenyl)-5-(pyridin-4-yl)-1*H*-imidazole (**7**).

Table 2. Geometrical Data of Compounds **4**−**7**

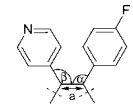

cmpd	a (Å)	α (deg)	β (deg)	d.a. (deg)	d.a. (deg)[a]
4	1.348[a]	128.7[a]	129.1[a]		59.63
5	1.396	132.6	129.2	46.61	60.50
6	1.363	136.3	129.8	49.51	58.93
7	1.393	134.2	129.7	44.66	58.36

[a] Determined by QM minimizations.

Table 3. Calculated AEPC and Hydrogen Binding Energy of Compounds **6** and **7**

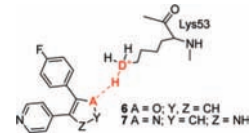

	6	**7**
AEPC (A)	−0.21 (O)	−0.58 (N3)
D−H···A	N−H···O	N−H···N3
HB binding energy	−11.50 kcal/mol	−25.05 kcal/mol

Results and Discussion

Biological Studies. The inhibitory potencies of compounds **4**, **5**, **6**, and **7** were evaluated using an isolated p38α MAP kinase assay[19] wherein SB203580 (**1**) was used as a reference. Table 1 compares the IC_{50} values of the cyclopentene **4**, pyrrole **5**, furan **6**, and imidazole **7** derivatives. The order of the inhibitory activity of the tested compounds **4**−**7** is imidazole ≫ pyrrole > furan ≫ cyclopentene derivative.

Computational Studies. The computational chemical calculation was carried out with the program package Jaguar from Schrödinger, Inc.

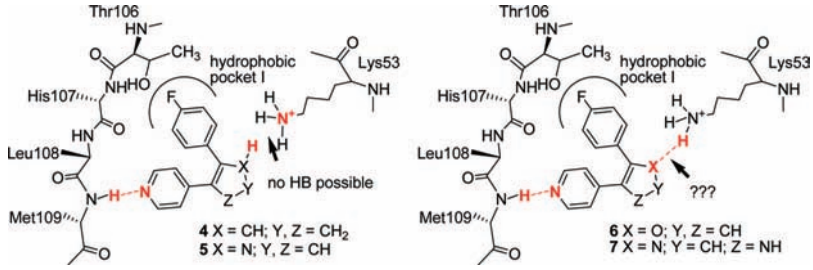

Figure 4. Possible interactions between compounds **4** and **5** (left) and **6** and **7** (right) and the ATP-binding site of p38α MAP kinase. No HB can be formed between X-H and the side chain of Lys53 in the case of compounds **4** and **5**. In the case of compounds **6** and **7**, the side chain of Lys53 is the donor of the HB.

Scheme 1. Preparation of 2-(4-fluorophenyl)-1-(pyridin-4-yl)cyclopentene (**4**)[a]

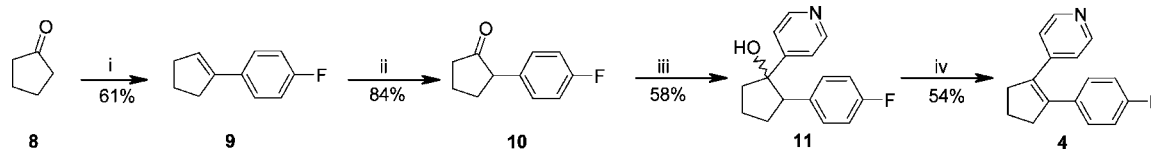

[a] Reagents: (i) 4-fluorophenylmagnesium bromide, ether, reflux; (ii) H_2O_2, formic acid; (iii) $NdCl_3 \cdot 2LiCl$, 1 h and then 2 equiv of PyMgCl·LiCl, 0 °C, 8−10 h; (iv) TsOH, H_2SO_4, toluene, reflux temperature, 1 h.

Scheme 2. Preparation of 2-(4-fluorophenyl)-3-(pyridin-4-yl)-1*H*-pyrrole (**5**) and 2-(4-fluorophenyl)-3-(pyridin-4-yl)furan (**6**)[a]

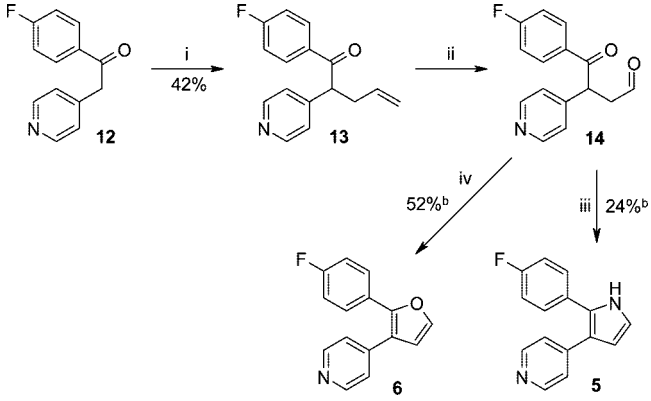

[a] Reagents: (i) NaHMDS, allyl bromide, THF, 0 °C; (ii) O_3, MeOH, 1.5 h, then Me_2S, 16 h at room temperature; (iii) NH_4OAc, HOAc, 115−120 °C; (iv) TsOH, AcOH, conc HCl, reflux temperature. [b]Yield over two steps.

Scheme 3. Preparation of 4-(4-fluorophenyl)-5-(pyridin-4-yl)-1*H*-imidazole (**7**)[a]

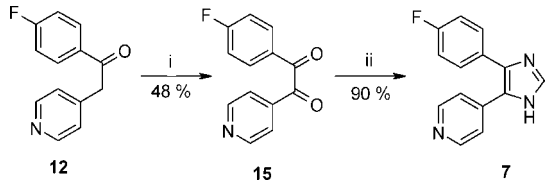

[a] Reagents: (i) SeO_2, HOAc, 95 °C; (ii) HCHO, NH_4OAc, AcOH, 5 min, 180 °C, 200 W, microwave.

Table 2 shows the common structural ground of these compounds determined by crystallographic data of compounds with heteroaromatic cores **5**,[20] **6**,[21] and **7**[22] as well as computational minimization of compounds **4**−**7**. The double bond between the two aromatic moieties of the nonaromatic cyclopentene scaffold is shorter compared to the heteroaromatic scaffolds. The pedant 4-fluorophenyl and pyridinyl moieties are in the same orientation.

The AEPCs of the derivatives **6** and **7** were calculated using density functional theory (DFT) with the B3LYP functional.[23] The AEPCs of the interesting atoms are −0.58 and −0.21 for imidazole-N3 and furan-O, respectively (Table 3).

The calculation of the HB binding energies from Lys53 to the furan and imidazole derivatives **6** and **7** was done with the Jaguar batch script hydrogen_bond.py (which is available in the Jaguar package).[24] The two compounds were first docked with an induced fit docking tool[25] into the X-ray structure of 1A9U.pdb.[4] The best docking poses were used for further calculations. For the calculation of the binding energies for the hydrogen-bonded complexes, we selected the fast mode, which uses the DFT energies instead of the LMP2 energies. Besides this, all torsions were frozen during optimizations. The HB binding energy of compounds **6** and **7** is −11.50 and −25.05 kcal/mol, respectively (Table 3).

Comparison. Both computational chemical calculation of the HB binding energy of the heterocyclic examples **6** and **7** to Lys53 and AEPC data show that the nitrogen atom is a better HB-acceptor than the oxygen atom. This is reflected in the inhibition of p38 MAP kinase. The imidazole derivative **7** is about five times more potent than the furan derivative **6**. The pyrrole **5** and the carbocyclic derivative **4**, which both are not able to form a HB to Lys53, show a significant difference in inhibition of p38 MAP kinase. The pyrrole **5** and the furan derivative **6** interact in different ways with the enzyme, since **5** is a HB donor and **6** an HB acceptor, but they show similar biological activity. These facts indicate an interaction between the N−H of pyrrole and Lys53. This could be caused by an intervening water molecule.

Conclusion

In this article, we present the synthesis and biological data of 2-(4-fluorophenyl)-1-(pyridin-4-yl)cyclopentene (**4**), 2-(4-fluorophenyl)-3-(pyridin-4-yl)-1*H*-pyrrole (**5**), and 2-(4-fluorophenyl)-3-(pyridin-4-yl)furan (**6**), and 4-(4-fluorophenyl)-5-(pyridin-4-yl)-1*H*-imidazole (**7**). The imidazole derivative **7** with the highest absolute value of AEPC at the N3 and lowest HB binding energy shows the best IC_{50}-value in our series. The cyclopentene derivative **4**, which is not able to form a HB to Lys53, shows a dramatic decrease in inhibitory activity of p38 MAP kinase (about 63 times less active than **7**). The pyrrol derivative **5**, which is not able to form a direct HB to Lys53,

shows interactions with the amino function of the side chain of Lys53. Maybe an intervening water molecule is playing a role.

Experimental Section

General. All commercially available reagents and solvents were used without further purification. The microwave reaction was performed on a CEM Discover system. Melting points were determined with a Büchi melting point B-545 and are thermodynamically corrected. NMR data were obtained on a Bruker Spectrospin AC 200 at ambient temperature. High-resolution spectra were obtained on a Thermo Finnigan TSQ70 instrument. The purity of the final compounds was determined by HPLC on a Hewlett-Packard HP 1090 Series II liquid chromatograph using a Betasil C8 column (150 mm × 4.6 mm i.d., dp = 5 μm, Thermo Fisher Scientific, Waltham, MA) at 230 and 254 nm employing a gradient of 0.01 M KH_2PO_4 (pH 2.3) and methanol as the solvent system with a flow rate of 1.5 mL/min; all final compounds have a purity of >98% (see Supporting Information for details).

2-(4-Fluorophenyl)-3-(pyridin-4-yl)-1*H*-pyrrole (5). Ammonium acetate (2.2 g, 34.9 mmol) was added to a solution of compound **14** (0.5 g) in glacial acetic acid (10 mL). The resulting mixture was heated to 115−120 °C for 2 h. The solvent was removed under reduced pressure, and the residue was diluted with ethyl acetate and aq $NaHCO_3$ solution. Solid Na_2CO_3 was added until effervescence ceased. The organic phase was washed with aq $NaHCO_3$ solution and brine and dried over Na_2SO_4, and the solvent was evaporated under reduced pressure to give crude **5**. The residue was dissolved in ethyl acetate (7 mL), filtered, and then purified by flash chromatography (SiO_2, petroleum ether/ethyl acetate 1−1 to 1−4). Yield 135 mg (24%, over two steps); Mp 260.8 °C; ^{1}H NMR (DMSO-d_6) 6.43−6.46 (m, 1H, C^4−H pyrrole), 6.92−6.95 (m, 1H, C^5−H pyrrole), 7.18−7.27 (m, 4H, C^3/C^5−H 4-F-Phe, C^3/C^5−H Pyr), 7.33−7.41 (m, 2H, C^2/C^6−H 4-F-Phe), 8.37 (dd, J_1 = 4.6 Hz, J_2 = 1.6 Hz, 2H, C^2/C^6−H Pyr), 11.47 (bs, 1H, NH); HRMS (EI): calculated for $C_{15}H_{11}FN_2$ 238.0906, found 238.0897.

The crystal structure of **5** has been proven by X-ray analysis: Enraf-Nonius CAD-4, Cu Kα, SIR92, SHELXL97. Further details of the crystal structure analysis are available in ref 20.

2-(4-Fluorophenyl)-3-(pyridin-4-yl)furan (6). Compound **14** (2.0 g) was treated with glacial acetic acid (10 mL) and conc HCl (30 mL) and then heated to reflux temperature for 4 h. The reaction mixture was cooled to room temperature and put into ice. A solution of K_2CO_3 was added until it became basic. The aqueous phase was extracted four times with ethyl acetate, and the combined organic layers were dried over Na_2SO_4 and filtered. The remaining solution was concentrated in vacuo and then purified by flash chromatography (SiO_2, petroleum ether/ethyl acetate 2−1 to 1−1) to give the furan derivative (1.15 g, 52%, over two steps) as a pale yellow solid. Mp 62.1 °C; ^{1}H NMR ($CDCl_3$) 6.55−6.56 (m, 1H, C^4−H furan), 6.95−7.03 (m, 2H, C^3/C^5−H 4-F-Phe), 7.24−7.27 (m, 2H, C^3/C^5−H Pyr), 7.41−7.48 (m, 3H, C^2/C^6−H 4-F-Phe, C^5−H furan), 8.54 (d, J = 4.7 Hz, 2H, C^2/C^6−H Pyr); HRMS (EI): calculated for $C_{15}H_{10}OFN$ 239.0746, found 239.0740.

The crystal structure of **6** has been proven by X-ray analysis: Enraf-Nonius CAD-4, Cu Kα, SIR92, SHELXL97. Further details of the crystal structure analysis are available in ref 21.

4-(4-Fluorophenyl)-5-(pyridin-4-yl)-1*H*-imidazole (7). Compound **15** (46 mg, 0.2 mmol), formaldehyde (15 μL, 0.2 mmol, 37% aq solution), ammonium acetate (154 mg, 2,0 mmol), and 1 mL of glacial acetic acid were combined in a reaction vial. The reaction vessel was heated in a CEM microwave reactor for 5 min at 180 °C (initial power 200 W), after which a stream of compressed air cooled the reaction vessel. The reaction mixture was added dropwise to a concentrated NH_4OH solution at 0 °C. The formed white/colorless precipitate was collected by filtration, washed with water, and dried. Yield 43 mg (90%); Mp 258.5 °C; ^{1}H NMR (DMSO-d_6) δ 7.22−7.31 (m, 2H, C^3/C^5−H 4-F-Phe), 7.38−7.41 (m, 2H, C^3/C^5−H Pyr), 7.45−7.52 (m, 2H, C^2/C^6 4-F-Ph), 7.86 (s, 1H, C^2−H imidazole), 8.45 (d, J = 5.8 Hz, 2H, C^2/C^6−H Pyr), 12.76 (bs, 1H, NH); HRMS (EI): calculated for $C_{14}H_{10}FN_2$ 239.0859, found 239.0765.

The crystal structure of **7** has been proven by X-ray analysis: Enraf-Nonius CAD-4, Cu Kα, SIR92, SHELXL97. Further details of the crystal structure analysis are available in ref 22.

Acknowledgment. The authors thank Dr. A. Liedtke for helpful discussions, S. Luik, K. Bauer, and M. Goettert for the assistance in biological testing, and the Alexander von Humboldt foundation (AvH) for funding.

Supporting Information Available: Full experimental procedures and analytical data for compounds **13**−**15** and **5**−**7**. This material is available free of charge via the Internet at http://pubs.acs.org.

References

(1) Kumar, S.; Boehm, J.; Lee, J. C. p38 MAP kinases: key signalling molecules as therapeutic targets for inflammatory diseases. *Nat. Rev. Drug Discovery* **2003**, *2*, 717–726.
(2) Lee, J. C.; Kassis, S.; Kumar, S.; Badger, A.; Adams, J. L. p38 mitogen-activated protein kinase inhibitors--mechanisms and therapeutic potentials. *Pharmacol. Ther.* **1999**, *82*, 389–397.
(3) Lee, M. R.; Dominguez, C. MAP kinase p38 inhibitors: Clinical results and an intimate look at their interactions with p38a protein. *Curr. Med. Chem.* **2005**, *12*, 2979–2994.
(4) Wang, Z.; Canagarajah, B. J.; Boehm, J. C.; Kassisa, S.; Cobb, M. H.; Young, P. R.; Abdel-Meguid, S.; Adams, J. L.; Goldsmith, E. J. Structural basis of inhibitor selectivity in MAP kinases. *Structure* **1998**, *6*, 1117–1128.
(5) Toledo, L. M.; Lydon, N. B.; Elbaum, D. The structure-based design of ATP-site directed protein kinase inhibitors. *Curr. Med. Chem.* **1999**, *6*, 775–805.
(6) Wrobleski, S. T.; Doweyko, A. M. Structural comparison of p38 inhibitor-protein complexes: A review of recent p38 inhibitors having unique binding interactions. *Curr. Top. Med. Chem. (Sharjah, United Arab Emirates)* **2005**, *5*, 1005–1016.
(7) Laufer, S. A.; Wagner, G. K. From Imidazoles to Pyrimidines: New Inhibitors of Cytokine Release. *J. Med. Chem.* **2002**, *45*, 2733–2740.
(8) Gallagher, T. F.; Seibel, G. L.; Kassis, S.; Laydon, J. T.; Blumenthal, M. J.; Lee, J. C.; Lee, D.; Boehm, J. C.; Fier-Thompson, S. M. Regulation of stress-induced cytokine production by pyridinylimidazoles; inhibition of CSBP kinase. *Bioorg. Med. Chem.* **1997**, *5*, 49–64.
(9) Fitzgerald, C. E.; Patel, S. B.; Becker, J. W.; Cameron, P. M.; Zaller, D.; Pikounis, V. B.; O'Keefe, S. J.; Scapin, G. Structural basis for p38a MAP kinase quinazolinone and pyridol-pyrimidine inhibitor specificity. *Nat. Struct. Biol.* **2003**, *10*, 764–769.
(10) de Laszlo, S. E.; Hacker, C.; Li, B.; Kim, D.; MacCoss, M.; Mantlo, N.; Pivnichny, J. V.; Colwell, L.; Koch, G. E.; Cascieri, M. A.; Hagmann, W. K. Potent, orally absorbed glucagon receptor antagonists. *Bioorg. Med. Chem. Lett.* **1999**, *9*, 641–646.
(11) de Laszlo, S. E.; Visco, D.; Agarwal, L.; Chang, L.; Chin, J.; Croft, G.; Forsyth, A.; Fletcher, D.; Frantz, B.; Hacker, C.; Hanlon, W.; Harper, C.; Kostura, M.; Li, B.; Luell, S.; MacCoss, M.; Mantlo, N.; O'Neill, E. A.; Orevillo, C.; Pang, M.; Parsons, J.; Rolando, A.; Sahly, Y.; Sidler, K.; Widmer, W. R.; O'Keefe, S. J. Pyrroles and other heterocycles as inhibitors of p38 kinase. *Bioorg. Med. Chem. Lett.* **1998**, *8*, 2689–2694.
(12) Steiner, T. Reviews: The hydrogen bond in the solid state. *Angew. Chem., Int. Ed.* **2002**, *41*, 48–76.
(13) Hao, M. H. Theoretical Calculation of Hydrogen-Bonding Strength for Drug Molecules. *J. Chem. Theory Comput.* **2006**, *2*, 863–872.
(14) Umeyama, H.; Morokuma, K. The origin of hydrogen bonding. An energy decomposition study. *J. Am. Chem. Soc.* **1977**, *99*, 1316–1332.
(15) Abu Thaher, B.; Koch, P.; Del Amo, V.; Knochel, P.; Laufer, S. A convenient synthesis of 1-(4-fluorophenyl)-2-(4-pyridyl)cyclopentene from cyclopentanone. *Synthesis* **2008**, 225–228.
(16) Qian, X.; Liang, G. B.; Feng, D.; Fisher, M.; Crumley, T.; Rattray, S.; Dulski, P. M.; Gurnett, A.; Leavitt, P. S.; Liberator, P. A.; Misura, A. S.; Samaras, S.; Tamas, T.; Schmatz, D. M.; Wyvratt, M.; Biftu, T. Synthesis and SAR studies of diarylpyrrole anticoccidial agents. *Bioorg. Med. Chem. Lett.* **2006**, *16*, 2817–2821.
(17) Boehm, J. C.; Smietana, J. M.; Sorenson, M. E.; Garigipati, R. S.; Gallagher, T. F.; Sheldrake, P. L.; Bradbeer, J.; Badger, A. M.; Laydon, J. T.; Lee, J. C.; Hillegass, L. M.; Griswold, D. E.; Breton, J. J.; Chabot-Fletcher, M. C.; Adams, J. L. 1-substituted 4-aryl-5-pyridinylimidazoles: a new class of cytokine suppressive drugs with low

5-lipoxygenase and cyclooxygenase inhibitory potency. *J. Med. Chem.* **1996**, *39*, 3929–3937.
(18) Wolkenberg, S. E.; Wisnoski, D. D.; Leister, W. H.; Wang, Y.; Zhao, Z.; Lindsley, C. W. Efficient synthesis of imidazoles from aldehydes and 1,2-diketones using microwave irradiation. *Org. Lett.* **2004**, *6*, 1453–1456.
(19) Laufer, S.; Thuma, S.; Peifer, C.; Greim, C.; Herweh, Y.; Albrecht, A.; Dehner, F. An immunosorbent, nonradioactive p38 MAP kinase assay comparable to standard radioactive liquid-phase assays. *Anal. Biochem.* **2005**, *344*, 135–137.
(20) Abu Thaher, B.; Koch, P.; Schollmeyer, D.; Laufer, S. 4-(2-(4-Fluorophenyl)-1H-pyrrol-3-yl)pyridine. *Acta Crystallogr., Sect. E: Struct. Rep. Online* **2009**, *E65*, o457.
(21) Abu Thaher, B.; Koch, P.; Schollmeyer, D.; Laufer, S. 4-(2-(4-Fluorophenyl)furan-3-yl)pyridine. *Acta Crystallogr., Sect. E: Struct. Rep. Online* **2009**, *E65*, o458.
(22) Koch, P.; Schollmeyer, D.; Laufer, S. 4-(5-(4-Fluorophenyl)-1*H*-imidazol-4-yl)pyridine. Acta Crystallogr., Sect. E: Struct. Rep. **2009**, *E65*, o573.
(23) Jaguar v 7.0; Schroedinger Inc., LLC: New York, NY, 2007.
(24) Jaguar v 7.5; Schroedinger Inc., LLC: New York, NY, 2008.
(25) Schroedinger Suite 2008, Induced Fit Docking Protocol; Glide version 5.0; Schroedinger, LLC: New York, 2005.

JM801467H